Australian Earthquake Engineering Society
2024 National Conference, 21-23 November 2024
Adelaide, South Australia

Prediction of Lateral Drift Behaviour of Precast Concrete Walls Using Finite Element Analysis

Xiangzhe Weng[1], Elisa Lumantarna[1], Ryan D. Hoult[2], Scott J. Menegon[3] and Nelson T. K. Lam[1]

1. *Department of Infrastructure Engineering, University of Melbourne, Parkville, VIC 3010, Australia.*
2. *Institute of Mechanics, Materials and Civil Engineering, UCLouvain, Louvain-la-Neuve, 1348, Belgium.*
3. *Department of Civil and Construction Engineering, Swinburne University of Technology, Hawthorn, VIC 3122, Australia*

Abstract

Finite element modelling has been widely applied by researchers and practitioners to evaluate the nonlinear behaviour of structural elements under earthquake actions. For the simulation of precast concrete walls, special considerations should be given to not only the modelling of the precast panels themselves but also the behaviour of connections between the panels and other structural elements. In addition, previous experimental testing on reinforced concrete walls has repeatedly shown that unconfined and non-validated finite element models can often grossly fail to reasonably predict structural performance. Therefore, this paper elaborates on a nonlinear and inelastic finite element model of typical precast reinforced concrete walls with grout tube connections. The force-displacement hysteresis response of these precast walls under in-plane reversed cyclic lateral loading was predicted from the finite element analysis. The numerical results were validated against experimental data available in the existing literature. The validated models can be employed to investigate the in-plane lateral drift behaviour of non-ductile and limited-ductile precast panels without confinement reinforcement, which are widely found in many low-to-moderate seismicity regions.

Keywords: total strain-based cracking, bond-slip, 2D plane stress, grouted dowel

1 Introduction

Precast reinforced concrete (RC) walls are becoming increasingly popular worldwide because of their advantages in better quality control, accelerating construction period and reduced environmental impacts. In recent years, there has been an increasing trend of adopting precast structural panels in new constructions of buildings in Australia. When assembling these precast walls on the construction site, grout tube connections are widely adopted as the horizontal connections between precast panels and foundations on the ground floor and between precast panels in the adjacent storeys. A 20-mm (typical) grout bedding layer is left between the adjoining elements for ease of alignment and a better stress distribution between the elements. If a longer wall length is desired, the panels can be joined together at the same storey by welded stitch plates. The typical detailing design of these precast panels and their connections can be found in Menegon et al. (2017), Seifi et al. (2016) and Weng et al. (2022).

Some researchers have investigated the lateral drift behaviour of precast RC panels with grout tube connections experimentally. One of the earliest studies of the seismic performance of precast walls in regions of lower seismicity was conducted by Crisafulli et al. (2002). They performed a reversed cyclic test of a precast panel connected to the foundation using grouted dowels. More experiments were performed in recent years. Seifi et al. (2019) tested seven precast walls with grout tube connections under reversed cyclic loads and investigated the effects of providing confining stirrups to the grout tubes. Menegon et al. (2020) prepared three precast core specimens using grout tube connections and welded stitch plates and determined the ultimate lateral behaviour of these cores under reversed cyclic loads. In general, for limited-ductile precast walls without confinement reinforcement at the wall boundaries, the lateral force-displacement behaviour of the precast panels showed a concentration of plasticity across the grout bedding layer at the wall base in the previous experiments (Crisafulli et al., 2002; Menegon et al., 2020; Seifi et al., 2019). Nevertheless, the study of these precast walls based on numerical simulations or finite element analysis (FEA) is relatively rare. Compared to cast-in-situ RC walls, the modelling of connections of precast elements (e.g., the grout tube connections and the grout bedding layer) is significantly more crucial and complicated. Some common modelling assumptions applied to the FEA of cast-in-situ walls, such as the perfect bond between reinforcing bars and concrete, cannot be applied to the modelling of precast walls (Weng et al., 2024).

An efficient and robust FE model can assess the structural behaviour of precast structural elements without the necessity of conducting expensive large-scale experimental tests. The model can also be utilised to investigate precast walls with varying design detailing and help engineers determine the appropriate detailing practices. Considering the paucity of studies on the investigation of the seismic performance of precast walls based on FEA, particularly for the precast walls with grout tube connections used in low-to-moderate seismicity regions (like Australia), this study proposes an FE modelling approach for evaluating these precast panels under in-plane reversed cyclic lateral loading. The numerical models are validated and calibrated using four experimental test units from the literature.

2 FE Modelling Strategy

2.1 Element Types

The FE program DIANA FEA (DIANA FEA B.V., 2024) is used to perform the nonlinear static analysis of precast walls with grout tube connections. The typical FE model of precast walls constructed in DIANA is shown in Figure 1. The two-dimensional regular plane stress (membrane) elements are used to model the loading beam, concrete panel, grout bedding layer and foundation block. Since the two-dimensional plane stress elements can only capture the in-plane stiffness, the out-of-plane behaviour of the precast walls (e.g., out-of-plane buckling) is out of the scope of this study. The horizontal and vertical wall reinforcement, as well as connection dowel bars, are modelled as discrete reinforcement in the concrete elements using truss bond-slip bar elements. The bond-slip reinforcement is a specialised type of reinforcement element in DIANA that incorporates truss elements for reinforcement and bond-slip interface elements between the reinforcement trusses and the adjoining concrete elements (Ferreira, 2024a).

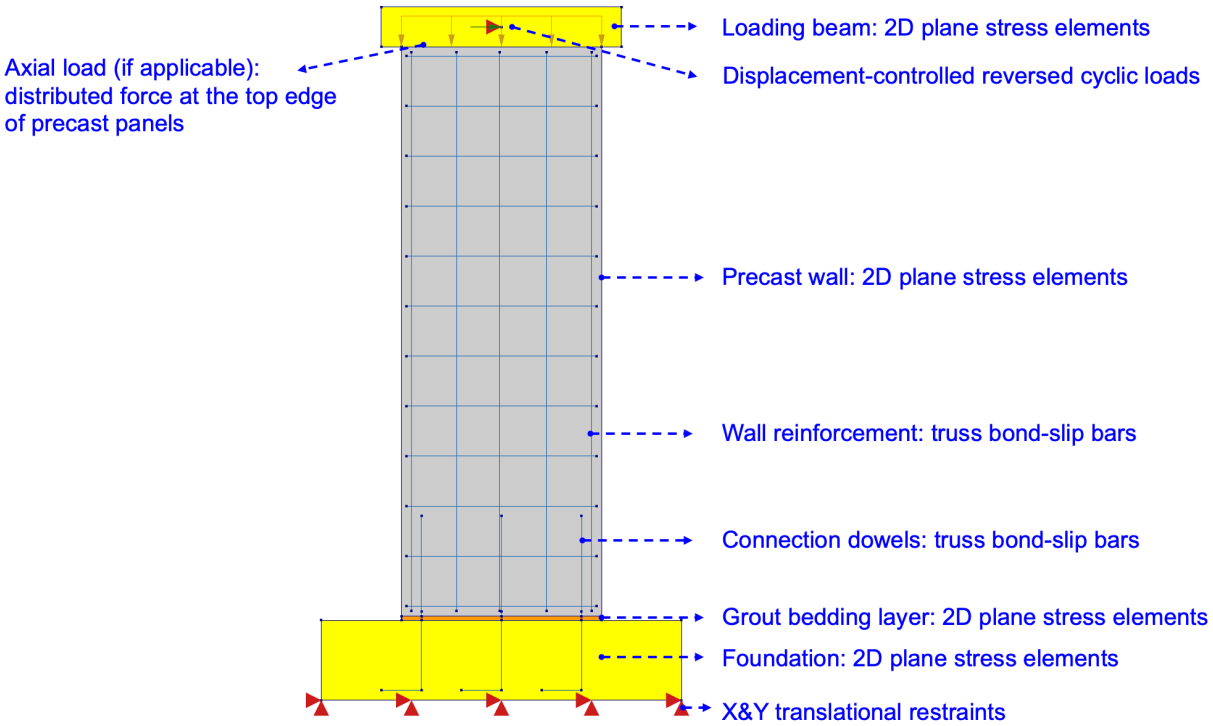

Figure 1. Illustration of the Typical Precast Wall Model in DIANA FEA

2.2 Material Models

The concrete in the foundation block and the precast panel is modelled by the Total Strain Crack Model in DIANA (Ferreira, 2024a). In the Total Strain Crack model, the concrete cracks are assumed to be distributed over the plane stress concrete elements, namely an assumption of smeared cracks (Ferreira, 2024a; Rots & Blaauwendraad, 1989). The width of the crack band is determined by Rots' method (Rots, 1988). In this study, the orientation of cracks is modelled by a fixed crack approach. The transfer of shear stress along the cracked surface due to aggregate interlock and dowel action of reinforcement is simulated by defining the shear retention factor for the concrete elements (Dabbagh & Foster, 2006; Ferreira, 2024a; Kupfer & Bulicek, 1991). A constant shear retention model is adopted in this study using a constant reduction factor of 0.01 to reduce the cracked shear stiffness. The same shear retention factor of 0.01 is adopted for grout elements of the grout bedding layer.

The uniaxial tensile and compressive stress-strain backbone curves of the Total Strain Crack concrete model are defined by the exponential tension softening model and parabolic compression model, respectively. The exponential model defines the tension softening behaviour based on the tensile fracture energy of concrete and the crack bandwidth. The tensile fracture energy (G_f^I) is estimated using the model proposed in fib Model Code 2010 for ordinary normal-weight concrete (International Federation for Structural Concrete [fib], 2013). The uniaxial concrete compressive behaviour is simulated by the parabolic model proposed by Feenstra (1993). The softening behaviour of the parabolic compressive model is associated with the compressive fracture energy (G_c). Based on the calibration of the FE models using experimental data of precast walls (Seifi et al., 2019), it is found that the compressive fracture energy can be estimated using Equation 1 proposed by Nakamura and Higai (2001). The reduction in the uniaxial compressive strengths due to concrete tensile cracking is determined by Vecchio-Collins 1993 – model B (Vecchio & Collins, 1993). In previous studies, the lower bound of Vecchio-Collins 1993 – Model B was taken as 0.4 to 0.6 (Botor, 2023; Ferreira, 2024b; Gotame et al., 2022; Miclăușoiu et al., 2024). From calibration and validation shown in Section 3, the wall models employing a lower bound of 0.5 for the reduction curve can attain a good match with the experimental results of all the precast panel specimens.

$$G_c = 250 G_f^I \qquad \text{Equation 1}$$

Where, G_c and G_f^I are concrete compressive fracture energy and tensile fracture energy, respectively.

The grout elements in the 20-mm grout bed layer are also simulated by the Total Strain Crack Model with the fixed crack approach. These grout elements are modelled as compression-only plane stress elements with 'zero' tensile strength and an ideal compressive model with the maximum stress being equal to the grout cubic compressive strength obtained from material tests. The elastic modulus of grout can be determined based on the product datasheet provided by the grout supplier. If no data is available, the grout elastic modulus might be estimated using the empirical formula proposed by Peng et al. (2022). Unlike some FE programs, such as VecTor2 (Wong et al., 2013), DIANA does not have a built-in 'compression-only' material model. Therefore, the tensile behaviour of grout elements is defined by a brittle tensile model with a small peak strength of 0.1 MPa and a residual strength of 0.01MPa to avoid convergence issues. The assumption of the 'negligible grout tensile strength' is based on the observation of premature cracking of the grout bedding layer in previous experimental tests of these precast walls under reversed cyclic loads (Menegon et al., 2020; Seifi et al., 2019). Furthermore, an ideal plasticity model is employed for the compressive behaviour of grout in the bedding layer in order to prevent the instability of the FE models because of the localised compressive failure of grout elements. Based on the validation provided in Section 3 of the paper, modelling the grout layer in this way can reasonably predict the flexural and rocking deformations of the walls. However, the limitation is that the sliding deformation of the walls at the base cannot be simulated using this approach.

The hysteretic behaviour of reinforcement, including the wall reinforcement and connection dowels, is modelled by the Dodd-Restrepo model (Dodd & Restrepo-Posada, 1995). The bond-slip behaviour of deformed bars in precast panels (i.e., wall horizontal and vertical reinforcement) and dowel bars in the foundation is simulated by the bond model provided in fib Model Code 2010 (International Federation for Structural Concrete [fib], 2013), namely the Eligehausen et al. (1983) model. The anchorage (i.e., 90-degree hooks) of reinforcement in the walls is modelled by defining a higher shear stiffness at the two end nodes of the truss element. The value of this increased shear stiffness is assumed to be the same as the normal stiffness of bond elements, which is approximately 100 times the ratio of concrete stiffness to the mesh size.

A new modelling approach has been developed by the authors to simulate the bond behaviour of dowel bars in grout tubes at the bottom of the precast panels based on the experimental pull-out tests of grout tube connections (Weng et al., 2023). As shown in Figure 2, the bond elements are divided into two regions: unconfined bond and confined bond. The bond stress-slip law for the unconfined bond region is defined using the model proposed by Steuck et al. (2009). The remaining length of dowel bars in grout tubes is modelled by a confined bond stress-slip law. The equation of this confined model is essentially the same as the bond model proposed by Eligehausen et al. (1983). However, the controlling bond stresses and slips of the model are determined using Equation 2 to Equation 7, which are calibrated using experimental data of pull-out tests of typical grout tube connections in precast walls in low-to-moderate seismicity regions (Weng et al., 2023). The updated equations will result in improved bond resistance and increased bond stiffness to account for the confinement effect provided by corrugated metal tubes. A reduced curve-fitting factor of 0.2 is proposed for the same purpose based on experimental results (Elsayed et al., 2019; Elsayed & Nehdi, 2017; Weng et al., 2023). In addition, since slippage between the metal spiral tube, concrete and grout was not observed in the experimental pull-out tests of the connections before the concrete was significantly split or crushed (Elsayed & Nehdi, 2017; Provost-Smith et al., 2019; Steuck et al., 2009; Weng et al., 2023), the metal tubes are neglected in the macro-model of precast walls. Therefore, the limitation of this simplified modelling approach is that the pull-out of tubes after extensive concrete spalling and crushing cannot be captured in the proposed FE models. However, this post-failure behaviour is not the focus of this study. In other words, the analysis will stop when

rebar ruptures (i.e., exceedance of the steel ultimate strain) or concrete crushing (i.e., 20% loss of lateral strength) occurs. Lastly, the steel loading beam at the top of precast panels can be modelled by a linear elastic model using the typical elastic modulus and Poisson's ratio of structural steel provided in design codes because the loading beam should not be yielded during the tests.

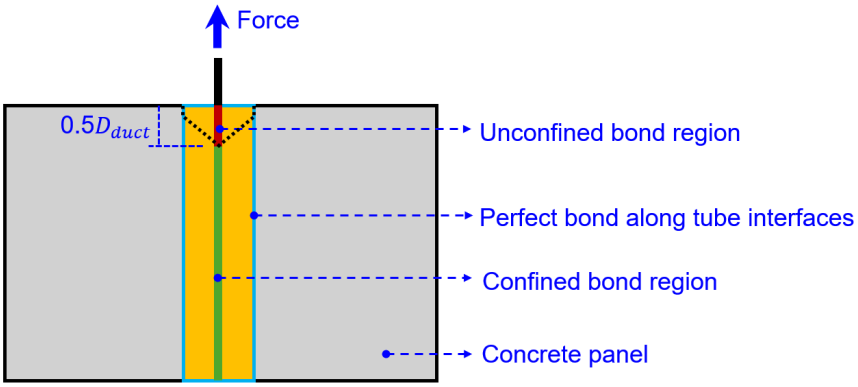

Figure 2. Proposed Modelling Approach for Bond Behaviour of Dowel Bars in Grout Tubes

$$\tau_{max} = 4.20 \cdot \sqrt{f_{g,cube}} \qquad \textit{Equation 2}$$

$$\tau_f = 0.49 \cdot \tau_{max} \qquad \textit{Equation 3}$$

$$s_1 = 0.0283 \cdot d_b \qquad \textit{Equation 4}$$

$$s_2 = 0.0417 \cdot d_b \qquad \textit{Equation 5}$$

$$s_3 = S \qquad \textit{Equation 6}$$

$$\alpha = 0.2 \qquad \textit{Equation 7}$$

Where, $f_{g,cube}$ is the grout cubic compressive strength in MPa; d_b is the bar diameter in mm; S is the bar lug spacing in mm; τ_{max}, τ_f, s_1, s_2 and s_3 are the stresses in MPa and slips in mm defining the shape of the Eligehausen et al. (1983) bond model.

2.3 Mesh Size

Based on a mesh sensitivity analysis, a fine mesh size leading to 40 elements along the wall length (i.e., $L_{wall}/40$) is adopted for meshing the quadrilateral elements (CQ16M) in the FE models. This mesh size is generally finer than the recommendations given in previous studies, such as half of the wall thickness recommended by Hoult et al. (2018) and Lu and Henry (2017) or $L_{wall}/14$ to $L_{wall}/16$ suggested in Palermo and Vecchio (2007). Therefore, an improved accuracy of the simulation results, particularly the cracking pattern and stress distribution, can be expected by using the proposed mesh size. In cases that using $L_{wall}/40$ results in a coarse mesh (e.g., for a large wall length), the maximum mesh size should not be greater than one-third of the wall thickness (Hoult & Almeida, 2022). It is noted that the adoption of fracture energy-based compressive and tensile models in this study can also help reduce the dependence of numerical results on the mesh size (Boer et al., 2014; Wani et al., 2022).

3 Validation of FE Models

The precast wall specimens tested by Seifi et al. (2019) were modelled in DIANA to validate and calibrate the proposed modelling approach. These models include the test units Wall 1,

Wall 4, Wall 5 and Wall 6 (abbreviated as SW1, SW4, SW5 and SW6 in the following section), in which the precast panels were unconfined at the wall boundaries (Seifi et al., 2019). The DIANA models were constructed based on the test setup and the design drawings provided by Seifi et al. (2019, 2021). The mechanical properties of materials measured from tests are summarised in Table 1 (Seifi et al., 2019). Since the original paper only provided the compressive strength of concrete, other concrete properties, such as Young's Modulus and tensile strength, are predicted using New Zealand concrete standard NZS 3101:2006 (Standards New Zealand, 2006), considering that the specimens were manufactured and tested in New Zealand (Seifi et al., 2019). Similarly, due to the lack of information in the original paper, the grout elastic modulus was estimated using the model proposed by Peng et al. (2022). The cyclic loadings applied to the FE models were displacement-controlled, with the designated drift levels reported by Seifi et al. (2019, 2021). The axial loads on SW5 and SW6 are defined based on the readings of axial load cells, as provided in Seifi et al. (2021). However, SW1 and SW4 were not subjected to additional axial loads in the experiment (Seifi et al. ,2019). Finally, using the meshing strategy discussed above, the FE models of the four walls are constructed in DIANA, as shown in Figure 3. The proposed mesh size of $L_{wall}/40$ resulted in a mesh width of 25 mm for SW1, SW4 and SW5, while a maximum size of 50 mm for SW6.

Table 1. Material Properties of Wall Specimens from Seifi et al. (2019)

	Concrete Compressive Strength (MPa)	Grout Compressive Strength (MPa)	Connection Dowel Bars			Wall Reinforcement		
			Yield strength (MPa)	Ultimate strength (MPa)	Strain at peak strength	Yield strength (MPa)	Ultimate strength (MPa)	Strain at peak strength
SW1	46	58	473	632	0.1	523	653	0.11
SW4	56	50	473	632	0.1	523	653	0.11
SW5	43	52	482	629	0.11	520	641	0.11
SW6	53	54	482	629	0.11	520	641	0.11

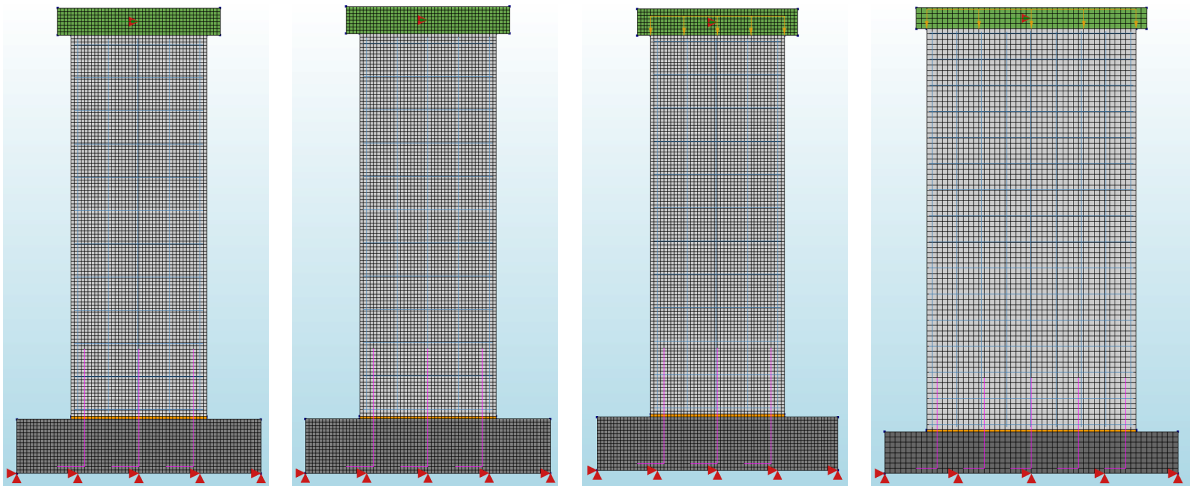

(a) SW1 (b) SW4 (c) SW5 (d) SW6

Figure 3. Geometry and Mesh of Precast Wall Models

Figure 4 presents the force-displacement results predicted by nonlinear FEA for the four wall specimens. As the proposed DIANA models cannot simulate the sliding deformation at the wall base, the experimental displacement cycles shown in the figure are adjusted by subtracting the wall base sliding deformations (measured in tests) from the lateral displacements recorded at the top of the walls in Seifi et al. (2021). In general, the numerical results of force-displacement curves match well with the experimental results presented in Seifi et al. (2019), particularly for SW1, SW5, and SW6. Regarding SW4, an early rupturing of the most left dowel bar (in tension) occurs in DIANA, but the discrepancy in peak strength between DIANA and the test result is acceptable. The prediction of a lower ultimate displacement from model SW4

is because the ultimate strain assigned to dowel bars in DIANA is likely lower than the actual rupture strain that might occur experimentally. Figure 5 illustrates a typical stress-strain curve of ductile deformed reinforcement. In the numerical analysis of steel reinforcement, it is a common practice to model the steel stress-strain curve up to the peak strength (i.e., point D) for conservative while ignoring the remaining elongation when necking occurs (i.e., branch DE) (Dodd & Restrepo-Posada, 1995). Therefore, the ultimate strain of the Dodd-Restrepo steel model used in DIANA was defined as the strain corresponding to the peak strength (i.e., point D). However, high-ductile deformed bars (e.g., the HD16 and HD12 bars used in the tests) could exhibit a significantly higher fracture strain (i.e., point E) than the peak strain (i.e., point D). For example, Russell (2013) reported a rupture strain of almost 0.14 and an even higher value of 0.2 was provided by Park (2003). Both values are considerably higher than the peak strain of 0.1 provided by Seifi et al. (2019) for connection reinforcement in SW4. Because the failure mode of SW4 is controlled by yielding and fracturing of dowel bars with almost no cracks observed in the panel experimentally (Seifi et al., 2019) and numerically (see Figure 6), increasing the ultimate steel strain of dowel bars in the FE model will considerably improve the ultimate displacement and make it closer to the experimental value. Similarly, in the FE model of SW6, the rupture of the outermost dowel bar in the extreme tension fibre happened shortly after the occurrence of concrete crushing (i.e., 20% loss of lateral strength, as shown in Figure 4), while in the experiment, the rebar rupture did not occur after crushing of the concrete (Seifi et al., 2019). The rupture of connection reinforcement observed numerically can be avoided if a greater ultimate steel strain is adopted in the model. However, it is worth noting that the strain corresponding to the peak force is used as the ultimate steel strain in DIANA models instead of the fracture strain also because the rupture strain of reinforcement was not reported in Seifi et al. (2019). Therefore, using a higher ultimate strain value in this case might result in different shear strengths being achieved numerically. Furthermore, as explained in Section 2.2, a limitation of the proposed simplified modelling approach (i.e., neglecting the corrugated tubes in the models) is that these numerical models cannot capture the pull-out failure of tubes after concrete crushing. According to Seifi et al. (2019), the failure mechanism of SW6 observed experimentally was initiated by concrete spalling and crushing, which eventually led to the pull-out of grout tubes. The slippage of tubes that occurred during the test could help mitigate the strain concentration in dowel bars at the grout bedding layer, therefore postponing the occurrence of dowel bar rupture. It can also be observed from Figure 4 that the rupture of the most left dowel bar in SW6 did not result in an abrupt drop in strength (as opposed to SW1 and SW4), and the force-displacement response shows a ductile failure behaviour with further progressive strength reduction when the wall was loaded to the next drift level. The strength softening behaviour of SW6 observed from the numerical force-displacement results matches reasonably well with the experimental results.

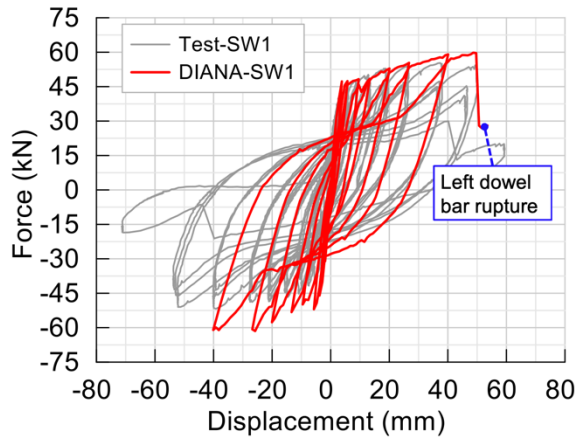

(a) SW1

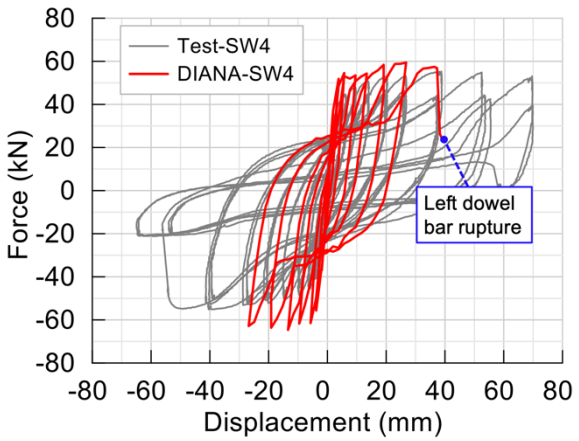

(b) SW4

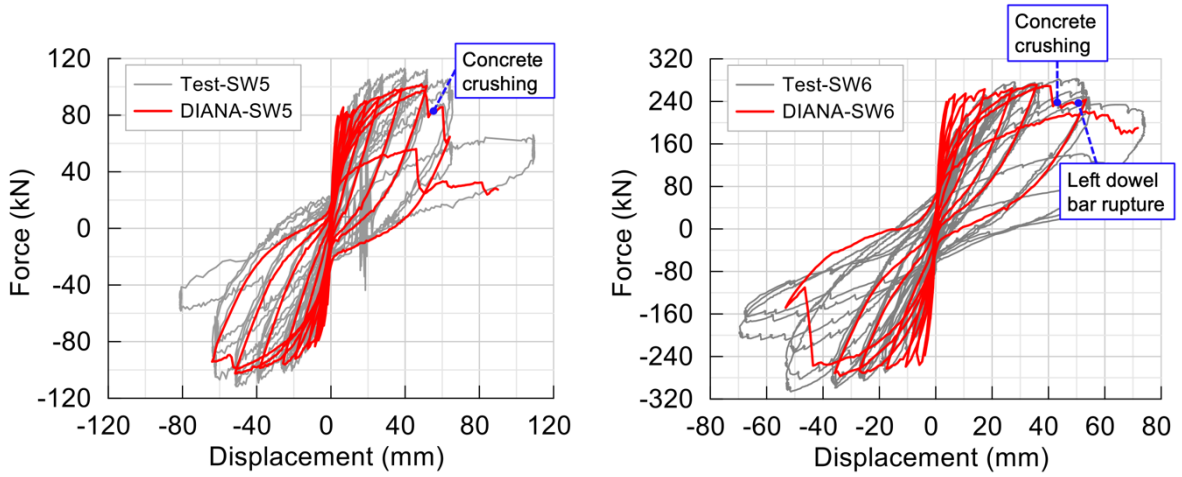

(c) SW5 (d) SW6

Figure 4. Lateral Force-Displacement Response of Precast Walls from DIANA and Comparison with Test Results (Seifi et al., 2019)

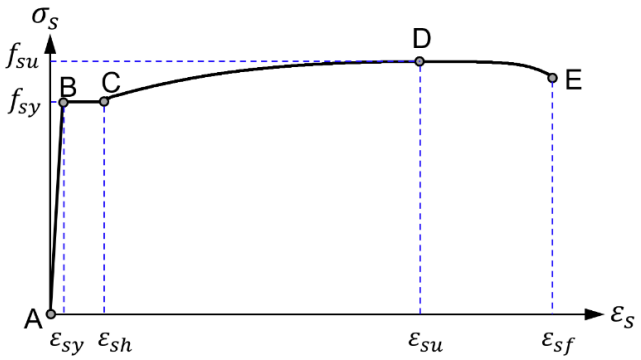

Figure 5. Stress-Strain Curve of Typical Ductile Reinforcement

The initial stiffness of SW6 is slightly overestimated in DIANA, as observed in Figure 4. This has been found to be associated with the tensile properties of concrete in DIANA. If a lower concrete strength or a brittle tensile model is used in DIANA, the initial stiffness of SW6 will match better with the test results. Therefore, it is possible that the tensile strength of SW6 estimated using the design equation in NZS 3101 gives a higher value than the actual tensile strength of the concrete specimen. Unfortunately, the concrete tensile strengths were not measured in the tests (Seifi et al., 2019). Similarly, the slightly overestimated strength of the negative cycles of model SW4 from FEA is also found to be associated with the concrete tensile model. A more symmetric response was found when a brittle concrete model was used in DIANA. However, using brittle concrete tensile models will result in underestimated lateral strength and compromised energy dissipation capacity in other walls. It is noted that the tensile behaviour of concrete has shown large scattering in previous material tests, which would be significantly affected by the concrete quality, aggregate size and environmental conditions (Japan Society of Civil Engineers, 2024). Therefore, considering that the overall force-displacement response of the walls from DIANA shows a good agreement with experimental results, the authors still recommend maintaining the use of the exponential tension softening model to simulate these precast panels. Despite some limitations, the proposed FE models are capable of predicting the flexural failure mechanism (i.e., rebar rupture or concrete crushing) and the hysteretic force-displacement response for all the specimens investigated here.

The cracking patterns from DIANA are shown in Figure 6 and compared with the crack distributions measured experimentally by Seifi et al. (2019). The proposed DIANA models can reasonably predict the distribution of cracks in the precast walls. For all the wall models, a

primary crack is formed at the base of the wall at the grout bedding layer. For SW1, SW5 and SW6, a secondary major crack was also formed at the location where the dowel bar ended. The formation of the secondary major crack indicates that the presence of dowel bars generated an over-strengthened region at the wall base, similar to the response of cast-in-situ walls with lapped splice connections (Menegon, 2018). By contrast, panel SW4 is basically uncracked during the numerical analysis, following the same pattern observed experimentally (Seifi et al., 2019). The increased wall thickness (i.e., 200 mm for SW4, while 150 mm for SW1, SW5 and SW6) and the double layer of wall reinforcement used in SW4 (other walls were singly reinforced) resulted in a significantly weaker section at the wall-to-foundation interface. It is worth noting that allowing the formation of secondary cracks is important for ensuring the performance of RC walls under earthquakes (Hoult, 2017; Hoult et al., 2018; Lu & Henry, 2017; Sritharan et al., 2014). A better distribution of concrete cracks will contribute to an improvement in the displacement capacity and ductility of precast walls. Several previous studies have assessed the minimum longitudinal reinforcement in cast-in-situ RC walls to allow the development of secondary cracks (Hoult, 2017; Hoult et al., 2018; Lu & Henry, 2017). It is also necessary to investigate how the reinforcement configuration in precast walls will affect the cracking pattern and displacement capacities, which will be the future focus of the authors.

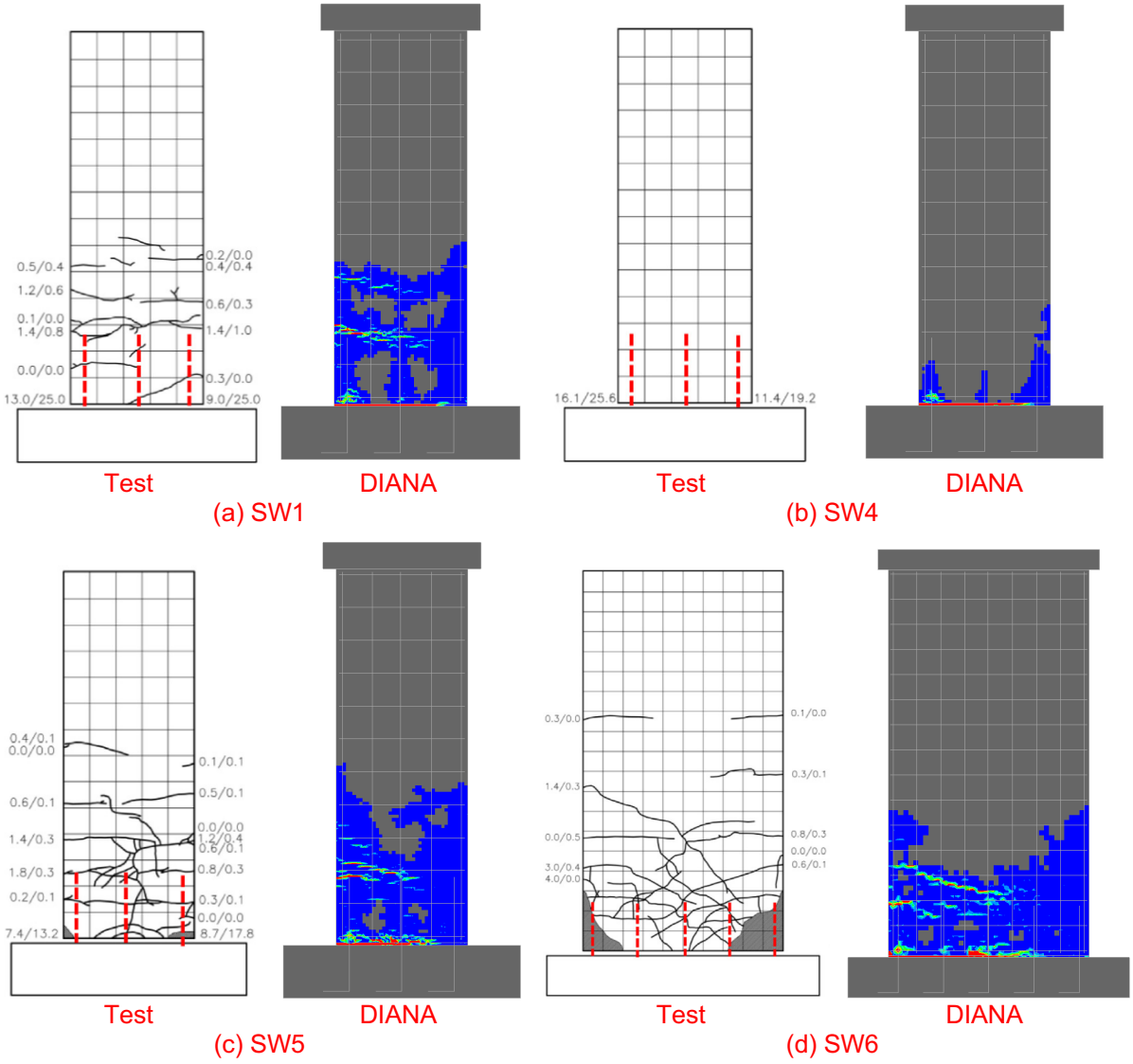

Figure 6. Cracking Patterns of Precast Walls from DIANA and Comparison with Test Results (Seifi et al., 2019)

4 Concluding Remarks

This study proposed a simplified finite element (FE) modelling approach for investigating the in-plane lateral drift behaviour of precast walls without confinement reinforcement, typically found in low-to-moderate seismicity regions. These precast walls utilise grout tube connections to join the vertical elements. A new bond model is proposed to simulate the pull-out behaviour of grout tube connections in these precast panels. The FE models are validated and calibrated using experimental data available in the existing literature. These models can reasonably predict the hysteretic force-displacement response and cracking patterns of these precast walls with sufficient accuracy. A further study conducted by the authors will be based on these validated FE models to investigate the impacts of typical detailing practices adopted in regions of lower seismicity on the seismic performance of these precast walls. However, it is necessary to mention that the proposed approach cannot simulate the out-of-plane instability of the walls, such as out-of-plane buckling of reinforcement. The sliding at the wall base is also neglected in the proposed approach. Future studies should aim to resolve these limitations. In addition, all the precast walls studied here have an aspect ratio of not less than 2. Therefore, the shear retention model adopted in this study should be recalibrated if the walls are primarily controlled by shear deformation (e.g., the wall's aspect ratio is less than 2).

5 Acknowledgement

This work was supported by the Melbourne Research Scholarship provided by the University of Melbourne. The authors sincerely acknowledge the financial support provided by the Charles Bubb Postgraduate Scholarship funded by the Australian Earthquake Engineering Society. The support by the Commonwealth through the Cooperative Research Centres (CRC) program (CRCPIX000240) is also gratefully acknowledged.

6 References

Almeida, J. P., Tarquini, D., & Beyer, K. (2016). Modelling Approaches for Inelastic Behaviour of RC Walls: Multi-level Assessment and Dependability of Results. *Archives of Computational Methods in Engineering*, *23*(1), 69–100. https://doi.org/10.1007/s11831-014-9131-y

Boer, A., Hendriks, M., den Uijl, J., Belletti, B., & Damoni, C. (2014). Nonlinear FEA guideline for modelling of concrete infrastructure objects. *Computational Modelling of Concrete Structures - Proceedings of EURO-C 2014*, *2*, 977–985. https://doi.org/10.1201/b16645-109

Botor, J. (2023). *Modelling the interface in concrete-to-concrete connections between precast girders and cast-in-situ top layers*. https://repository.tudelft.nl/islandora/object/uuid%3Ae556509b-49c9-42ed-b411-8d7579edfc2b

Crisafulli, F. J., Restrepo, J. I., & Park, R. (2002). Seismic Design of Lightly Reinforced Precast Concrete Rectangular Wall Panels. *PCI Journal*, *47*, 104–121. https://doi.org/10.15554/pcij.07012002.104.121

Dabbagh, H., & Foster, S. J. (2006). A Smeared—Fixed Crack Model for FE Analysis of RC Membranes Incorporating Aggregate Interlock. *Advances in Structural Engineering*, *9*(1), 91–102. https://doi.org/10.1260/136943306776232927

de Putter, A., Hendriks, M. A. N., Rots, J. G., Yang, Y., Engen, M., & van den Bos, A. A. (2022). Quantification of the resistance modeling uncertainty of 19 alternative 2D nonlinear finite element approaches benchmarked against 101 experiments on reinforced concrete beams. *Structural Concrete*, *23*(5), 2895–2909. https://doi.org/10.1002/suco.202100574

DIANA FEA B.V. (2024). *DIANA Release 10.9* [Computer software]. DIANA FEA BV. https://dianafea.com/

Dodd, L. L., & Restrepo-Posada, J. I. (1995). Model for Predicting Cyclic Behavior of Reinforcing Steel. *Journal of Structural Engineering*, *121*(3), 433–445. https://doi.org/10.1061/(ASCE)0733-9445(1995)121:3(433)

Eligehausen, R., Popov, E. P., & Bertero, V. V. (1983). *Local Bond Stress-Slip Relationship of Deformed Bars under Generalised Excitations—Experimental Results and Analytical Model* (No. UCB/EERC-83/23). Earthquake Engineering Research Center, University of California, Berkeley. https://doi.org/10.18419/opus-8473

Elsayed, M., & Nehdi, M. L. (2017). Experimental and analytical study on grouted duct connections in precast concrete construction. *Materials and Structures*, *50*(4). https://doi.org/10.1617/s11527-017-1056-0

Elsayed, M., Nehdi, M. L., & Ghrib, F. (2019). Predicting Behavior of Grouted Dowel Connections Using Interfacial Cohesive Elements. *Applied Sciences*, *9*(11), 2344. https://doi.org/10.3390/app9112344

Feenstra, P. H. (1993). *Computational Aspects of Biaxial Stress in Plain and Reinforced Concrete*. https://repository.tudelft.nl/islandora/object/uuid%3Afaf2fd16-1c43-4711-b783-9e8e00d10c21

Ferreira, D. (2024a). *DIANA User's Manuals (DIANA 10.9)*. DIANA FEA BV. https://manuals.dianafea.com/d109/?lang=en

Ferreira, D. (2024b). *Verification report (DIANA 10.9)*. DIANA FEA bv. https://manuals.dianafea.com/d109/en/1092500-1092500-verification-report.html

Gotame, M., Franklin, C. L., Blomfors, M., Yang, J., & Lundgren, K. (2022). Finite element analyses of FRP-strengthened concrete beams with corroded reinforcement. *Engineering Structures*, *257*, 114007. https://doi.org/10.1016/j.engstruct.2022.114007

Hoult, R. D. (2017). Minimum Longitudinal Reinforcement Requirements for Boundary Elements of Limited Ductile Walls for AS 3600. *Electronic Journal of Structural Engineering*, *17*, 43–52. https://doi.org/10.56748/ejse.17218

Hoult, R. D., & de Almeida, J. P. (2022). From experimental strain and crack distributions to plastic hinge lengths of RC walls with SMA rebars. *Engineering Structures*, *268*, 114731. https://doi.org/10.1016/j.engstruct.2022.114731

Hoult, R. D., Goldsworthy, H., & Lumantarna, E. (2018). Plastic Hinge Length for Lightly Reinforced Rectangular Concrete Walls. *Journal of Earthquake Engineering*, *22*(8), 1447–1478. https://doi.org/10.1080/13632469.2017.1286619

International Federation for Structural Concrete [fib]. (2013). *Fib Model Code for Concrete Structures 2010* (Berlin). Ernst & Sohn.

Japan Society of Civil Engineers. (2024). *The Japan Society of Civil Engineers (JSCE) Standard Specifications for Concrete Structures*.

Kupfer, H., & Bulicek, H. (1991). Comparison of Fixed and Rotating Crack Models in Shear Design of Slender Concrete Beams. In D. E. Grierson, A. Franchi, & P. Riva (Eds.), *Progress in Structural Engineering* (pp. 129–138). Springer Netherlands. https://doi.org/10.1007/978-94-011-3616-7_8

Lu, Y., & Henry, R. S. (2017). Numerical modelling of reinforced concrete walls with minimum vertical reinforcement. *Engineering Structures*, *143*, 330–345. https://doi.org/10.1016/j.engstruct.2017.02.043

Menegon, S. J. (2018). *Displacement Behaviour of Reinforced Concrete Walls in Regions of Lower Seismicity* [Doctoral Dissertation, Swinburne University of Technology]. https://researchbank.swinburne.edu.au/items/f0fa424a-fd0e-44b1-958a-5f32b5121711/1/

Menegon, S. J., Wilson, J. L., Lam, N. T., & Gad, E. F. (2020). Experimental assessment of the ultimate performance and lateral drift behaviour of precast concrete building cores. *Advances in Structural Engineering*, *23*(12), 2597–2613. https://doi.org/10.1177/1369433220919077

Menegon, S. J., Wilson, J. L., Lam, N. T. K., & Gad, E. F. (2017). RC walls in Australia: Reconnaissance survey of industry and literature review of experimental testing. *Australian Journal of Structural Engineering*, *18*(1), 24–40. https://doi.org/10.1080/13287982.2017.1315207

Miclăușoiu, D.-A., Nedelcu, M., & Blanksvärd, T. (2024). Experimental and numerical analysis of different vertical connections of precast shear walls with special regard towards deformability. *Structural Concrete*, *25*(1), 85–110. https://doi.org/10.1002/suco.202300429

Nakamura, H., & Higai, T. (2001). Compressive Fracture Energy and Fracture Zone Length of Concrete. *Modeling of Inelastic Behavior of RC Structures Under Seismic Loads*.

Palermo, D., & Vecchio, F. J. (2007). Simulation of Cyclically Loaded Concrete Structures Based on the Finite-Element Method. *Journal of Structural Engineering*, *133*(5), 728–738. https://doi.org/10.1061/(ASCE)0733-9445(2007)133:5(728)

Park, B. (2003). Some controversial aspects of the seismic design of reinforced concrete building structures. *Bulletin of the New Zealand Society for Earthquake Engineering*, *36*, 165–188. https://doi.org/10.5459/bnzsee.36.3.165-188

Peng, G., Hu, X., Niu, D., & Zhong, S. (2022). Complete Stress–Strain Relations of Early-Aged Cementitious Grout under Compression: Experimental Study and Constitutive Model. *Materials*, *15*(3), Article 3. https://doi.org/10.3390/ma15031238

Provost-Smith, D. J., Elsayed, M., & Nehdi, M. L. (2019). Investigation of Grouted Dowel Connections for Precast Wall Construction. *ACI Structural Journal*, *116*(1). https://doi.org/10.14359/51710860

Rots, J. G. (1988). *Computational modeling of concrete fracture | TU Delft Repository* [Doctoral Dissertation]. http://resolver.tudelft.nl/uuid:06985d0d-1230-4a08-924a-2553a171f08f

Rots, J. G., & Blaauwendraad, J. (1989). *Crack Models for Concrete: Discrete or Smeared? Fixed, Multi-Directional or Rotating?* HERON.

Russell, A. P. (2013). *Strain hardening of reinforcement in concrete buildings during earthquakes*. Queenstown, New Zealand. https://cdn.ymaws.com/concretenz.org.nz/resource/resmgr/docs/conf/2013/s5_p4.pdf

Seifi, P., Henry, R. S., & Ingham, J. M. (2016). Panel connection details in existing New Zealand precast concrete buildings. *Bulletin of the New Zealand Society for Earthquake Engineering*, *49*(2), 190–199. https://doi.org/10.5459/bnzsee.49.2.190-199

Seifi, P., Henry, R. S., & Ingham, J. M. (2019). In-plane cyclic testing of precast concrete wall panels with grouted metal duct base connections. *Engineering Structures*, *184*, 85–98. https://doi.org/10.1016/j.engstruct.2019.01.079

Seifi, P., Henry, R. S., & Ingham, J. M. (2021). *University of Auckland: Precast Concrete Wall Tests—Grouted Connections* [Dataset]. DesignSafe-CI; DesignSafe-CI. https://doi.org/10.17603/ds2-trtb-5r56

Sritharan, S., Beyer, K., Henry, R. S., Chai, Y. H., Kowalsky, M., & Bull, D. (2014). Understanding Poor Seismic Performance of Concrete Walls and Design Implications. *Earthquake Spectra*, *30*(1), 307–334. https://doi.org/10.1193/021713eqs036m

Standards New Zealand. (2006). *Concrete structures standard* (NZS 3101.1 & 2:2006 (Inc A1, A2 A3)). https://www.standards.govt.nz

Steuck, K. P., Eberhard, M. O., & Stanton, J. F. (2009). Anchorage of Large-Diameter Reinforcing Bars in Ducts. *ACI Structural Journal*, *106*(4). https://doi.org/10.14359/56616

Vecchio, F. J., & Collins, M. P. (1993). Compression Response of Cracked Reinforced Concrete. *Journal of Structural Engineering*, *119*(12), 3590–3610. https://doi.org/10.1061/(ASCE)0733-9445(1993)119:12(3590)

Wani, F. M., Khan, M. A., & Vemuri, J. (2022). 2D nonlinear finite element analysis of reinforced concrete beams using total strain crack model. *Materials Today: Proceedings*, *64*, 1305–1313. https://doi.org/10.1016/j.matpr.2022.04.196

Weng, X., Lumantarna, E., Hoult, R. D., & Lam, N. T. K. (2022). *A survey focusing on precast reinforced concrete walls in Australia with some preliminary analyses*. Proceedings of the Australian Earthquake Engineering Society 2022 National Conference, Melbourne, Australia. https://aees.org.au/wp-content/uploads/2022/11/A-survey-focusing-on-precast-reinforced-concrete-walls-in-Australia-with-some-preliminary-analyses.pdf

Weng, X., Lumantarna, E., Hoult, R. D., & Lam, N. T. K. (2024). A Simplified Finite Element Model of Grouted Duct Connections in Precast Reinforced Concrete Walls. In N. Chouw & C. Zhang (Eds.), *Proceedings of the 26th Australasian Conference on the Mechanics of Structures and Materials* (pp. 311–322). Springer Nature. https://doi.org/10.1007/978-981-97-3397-2_28

Weng, X., Menegon, S. J., Lumantarna, E., Hoult, R. D., Sofi, M., & Lam, N. T. (2023). Pullout Tests of Grout Tube Connections in Limited Ductile Precast Reinforced Concrete Walls. *Proceedings of the Australian Earthquake Engineering Society 2023 National Conference*.

Wong, P. S., Vecchio, F. J., & Trommels, H. (2013). *VecTor2 & Formworks user's manual—Second edition*. http://vectoranalysisgroup.com/user_manuals/manual1.pdf